



ISSN: 0067-2904

Oil Spill Removal from Water Surfaces using Zinc Ferrite Magnetic Nanoparticles as A Sorbent Material

Ibrahim A. Amar^{1*}, Sawsan I. Faraj¹, Mabroukah A. Abdulqadir¹, Ihssin A. Abdalsamed¹, Fatima A. Altohami¹, Mohammed A. Samba²

¹Department of Chemistry, Faculty of Science, Sebha University, Sebha, Libya

²Department of Oil and Gas Engineering, Faculty of Energy and Mining Engineering, Sebha University, Sebha, Libya

Received: 28/1/2020

Accepted: 25/7/2020

Abstract

In this study, zinc ferrite magnetic nanoparticles ($ZnFe_2O_4$, ZFO MNPs) were employed as a sorbent for the removal of oil spill from water surfaces. ZFO MNPs were synthesized via a sol-gel process and characterized by Fourier transform infrared spectroscopy (FTIR) and X-ray powder diffraction (XRD). Both the apparent density and magnetic force were determined. ZFO MNPs presented a considerable magnetic force (40.22 mN) and an adequate density (0.5287 g/cm^3), which are important for the magnetic separation and flotation. Four oil samples (gasoline engine oil, crude oil, used motor oil and diesel engine oil) were used to investigate the gravimetric oil removal capability of ZFO MNPs. The oil sorption capacities were found to be 23.00-6.13, 27.65-7.42, 22.62-7.01 and 30.54-9.93 g/g for crude, diesel engine, gasoline engine, and used motor oil, respectively. The current findings demonstrate that ZFO MNPs exhibit good properties (e.g., magnetic and density) and can be used as a sorbent for oil spill cleaning-up from water surfaces.

Keywords: Spinel ferrite nanoparticles; magnetic nanosorbent; oil sorption; gravimetric oil removal.

إزالة بقع الزيت من سطح الماء باستخدام حبيبات الزنك فيرايت النانوية المغناطيسية كمادة مازة

إبراهيم علي عمار^{1*}، سوسن إدريس فرج¹، مبروكة الصالحين عبدالقادر¹، حسين أبوبكر

عبدالصمد¹، فاطمة علي التوهامي¹، محمد الشريف صمبة²

¹قسم الكيمياء، كلية العلوم، جامعة سبها، سبها، ليبيا

²قسم هندسة النفط و الغاز، كلية هندسة الطاقة و التعدين، جامعة سبها، سبها، ليبيا

الخلاصة

في هذه الدراسة، تم استخدام حبيبات الزنك فيرايت النانوية المغناطيسية ($ZnFe_2O_4$, ZFO) لإزالة بقع الزيت من سطح الماء. تم استخدام طريقة المحلول-هلام (Sol-gel) لتحضير حبيبات الزنك فيرايت و تم تشخيصها بواسطة طيف حيود الأشعة السينية (XRD) و طيف إمتصاص الأشعة تحت الحمراء (FTIR). كما تم تقدير القوة المغناطيسية و الكثافة الظاهرية لحبيبات الزنك فيرايت النانوية. و كانت قيمة القوة المغناطيسية تساوي (40.22 ملي نيوتن) و الكثافة تساوي (0.5287 جم/سم^3)، و هذه الخواص ذات أهمية كبيرة حيث انها تساعد في عملية الفصل المغناطيسي و الطفو لحبيبات الزنك فيرايت. الازالة الوزنية لحبيبات

*Email: ibr.amar@sebhau.edu.ly

الزنك فيرايت النانوية المغناطيسية تم دراستها باستخدام النفط الخام، زيت السيارات المستعمل، زيت محركات سيارات الديزل و زيت محركات سيارات الجازولين كمأمثلة على ملوثات المياه. سعة إمتزاز حبيبات الزنك فيرايت النانوية للزيوت كانت 6.13-23.00، 7.42-27.65، 7.01-22.62 و 9.93-30.54 جم/جم للنفط الخام، زيت محركات سيارات الديزل، زيت محركات سيارات الجازولين و زيت السيارات المستعمل، على التوالي. من هذه الدراسة يتضح أن لحبيبات الزنك خواص جيدة (المغناطيسية و الكثافة) و يمكن إستخدامها كمادة مازة لإزالة بقع الزيت من سطح الماء.

1. Introduction

Oil has become an essential element to our modern industrial society and our daily life. In fact, the worldwide production and consumption of oil and petroleum products (*e.g.*, plastics, chemical feedstocks, and fertilizers) are increasing, and oil pollution risk is increasing consequently [1]. In oil industry, spills or leakages can occur during various steps, including oil exploration, production activities, transportation, and storage [1, 2]. It was estimated that about 400.000 tons of oil are spilt annually [3]. For instance, one of the biggest oil spills in human history occurred in 1991 during Kuwait oil fire, at which one billion tons of oil was burnt and poisonous gases were released into the environment [4]. Another oil spill accident occurred in 2010 in the Deep-water of Gulf of Mexico and released approximately 206 million gallons of petroleum products into the sea [4, 5]. Oil spills in water bodies (seas, oceans, *etc.*) and land can threat the environment, as they have detrimental effects on marine life as well as human and animal health [1, 2, 4]. In disaster management, oil spillage cleanup is one of the most expensive processes. For example, in the USA, from 16 to 20 dollars per gallon is the estimated average cost for spilled oil cleanup [4]. Therefore, there is an urgent need to develop economic, effective, and feasible technologies for oil spills cleaning.

Currently, there are different methods for spilled oil cleanup, such as physical (*e.g.*, skimmers and sorption) [6-8], chemical (*e.g.*, dispersion and in-situ burning) [9, 10], and bioremediation [11]. Among these, the oil sorption technique is preferred due to its unique properties, such as environmental-friendliness, availability of various sorbents, cost-effectiveness, low energy consumption, high efficiency, *etc.* [12, 13]. Nanomaterials, in particular magnetic nanoparticles (MNPs), were widely employed as sorbent materials for oil spillage cleanup due to their diverse structure, ease of functionalization, high surface area, high oil sorption capacity, moderate saturation magnetization, high chemical, thermal and mechanical stabilities, ease of separation and recovery under the influence of an external magnetic field, *etc.* [14-16]. In addition, nanomaterials, including spinel ferrites, are synthesized using several methods, such as sol-gel, hydrothermal, co-precipitation, thermal decomposition, microemulsion, solvothermal, microwave-assisted, and sonochemical [14, 17, 18]. Based on the aforementioned properties of MNPs, spinel ferrites (SFs) have found widespread applications in many fields, including adsorption [19-21], magnetic devices [22], biomedicine [23], ammonia synthesis [24, 25], photocatalysis [26], sensors [27], *etc.* In terms of oil spillage removal, different spinel ferrites and their corresponding nanocomposites were used as oil sorbent materials, such as PVDF/CoFe₂O₄ [2], CoFe_{1.9}Zn_{0.1}O₄ [8], PS/NiFe₂O₄ [28], and CoFe₂O₄/sawdust [29]. However, oil removal using zinc ferrite magnetic nanoparticles (ZnFe₂O₄ MNPs) has not been reported yet. Therefore, the main focus of the present work is to investigate the capabilities of ZnFe₂O₄ MNPs for oil spillage cleanup from water surfaces.

2. Experimental Part

2.1 Materials and Chemicals

The Libyan crude oil sample was received from Amal oil field, Harouge oil operations, Libya. A used motor oil sample was collected from car oil change shops. Gasoline and diesel engine oils were purchased from local shops. Zinc acetate dihydrate ((CH₃COO)₂Zn·2H₂O, 98-102%) was purchased from VWR Chemicals. Iron (III) nitrate nonahydrate (Fe(NO₃)₃·9H₂O, > 98%) was received from Berck and Scientific Supplies. Citric acid (C₆H₈O₇, > 99.5%) was obtained from Labkem. Ammonia solution (35%) was purchased from Scharlau. Ethylenediaminetetraacetic acid (EDTA, C₁₀H₁₈N₂O₈, 99%) was supplied by Serva. All chemicals were used as received, with no purification.

2.2 Synthesis of ZnFe₂O₄ Magnetic Nanoparticles

ZFO MNPs were synthesized using a sol-gel process, as described elsewhere [30]. In brief, calculated amounts of (CH₃COO)₂Zn·2H₂O and Fe(NO₃)₃·9H₂O were dissolved in deionized water. Then, EDTA and citric acid were added to the metal nitrates solution as complexing agents with a

ratio of citric acid : EDTA : metal cations of 1.5 : 1 : 1. Afterward, a diluted ammonia solution was added to adjust the pH of the mixed solution to around 6. At this pH value, EDTA dissolves completely. The mixture was magnetically stirred and evaporated on a hotplate before being converted into a solid product (dried gel). Finally, the dried gel was calcined in air at 600 °C for 2 h to obtain ZFO MNPs. The sol-gel process used for ZFO MNPs synthesis is represented in Figure-1.

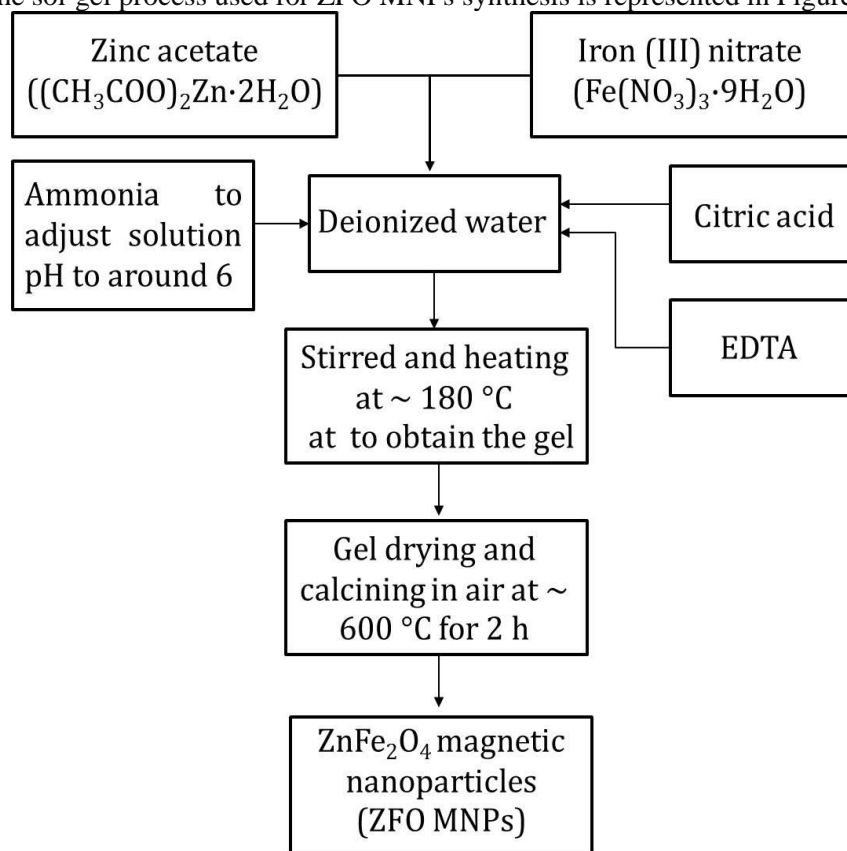


Figure 1- Flowchart representing ZFO MNPs synthesis using a sol-gel process

2.3 Characterization of ZFO MNPs and oil samples

Philips – PW 1800 X-ray powder diffractometer with Cu-K α radiation ($\lambda = 1.54186 \text{ \AA}$) was used to record the XRD patterns of ZFO MNPs at room temperature. The lattice parameters (a), unit cell volume (V_{cell}), X-ray density (ρ_{XRD}), crystallite size (D), and the specific surface area (S_{XRD}) of the prepared magnetic nanoparticles were estimated using Equations (1) to (5), respectively [31, 32];

$$a = d_{hkl} \sqrt{h^2 + k^2 + l^2} \quad (1)$$

$$V_{cell} = a^3 \quad (2)$$

$$\rho_{XRD} = \frac{ZM}{N_A V_{cell}} \quad (3)$$

$$D = \frac{0.9 \lambda}{\beta \cos \theta} \quad (4)$$

$$S_{XRD} = \frac{6000}{D \cdot \rho_{XRD}} \quad (5)$$

where d is the interplanar distance, hkl are the Miller indices, Z is the number of molecules per formula unit ($Z = 8$ for spinel system), N_A is the Avogadro's number, M is the molecular weight of the sample, β (in radian) is the full width at half maximum (FWHM) of the peak, λ is the wavelength of the X-ray, and θ is the Bragg angle.

Nicolet 380 spectrometer was used to perform the FTIR analysis of ZFO MNPs in the wavenumber range of 400-4000 cm^{-1} using the KBr disc method. Bruker Tensor 27 spectrometer was used to record the FTIR spectra of the oil samples in the wavenumber range of 600-4000 cm^{-1} using the Attenuated Total Reflectance mode (ATR).

The apparent density (ρ_a) of ZFO MNPs was measured as described elsewhere [33]. In this experiment, the weight and volume of ZFO MNPs inside a 10 mL graduated cylinder were determined. Then, the following equation was used to estimate the apparent density [34];

$$\rho_a \text{ (g/cm}^3\text{)} = \frac{W_s}{V_s} \quad (6)$$

where V_s and W_s are the volume and the weight of ZFO MNPs inside a 10 mL graduated cylinder, respectively.

The magnetic force (F_m) test of ZFO MNPs was carried out using an electromagnet, triple beam balance (700/800 Series, OHAUS®), Teslameter (LEYBOLD, DIDACTIC GMBH), and power supply (Hochstrom-Netzerat, LEYBOLD). The ZFO MNPs was subjected to a magnetic field. The intensity of the magnetic field was increased by applying an electric current ranging from 0 to 0.9 A. Then, the F_m (mN) was estimated using the following equation [35];

$$F_m = \Delta m \times g \quad (7)$$

where Δm is the apparent mass variation of ZFO MNPs in the presence of magnetic field and g is the acceleration of gravity.

2.4 Oil Removal Experiments

The oil removal study was carried out using the gravimetric oil removal method, as described elsewhere [35, 36]. In this experiment, a 25 mL beaker was filled with a 20 mL of seawater. To this beaker, a known amount of oil sample under investigation (crude, diesel, gasoline, and used oil) was spilled on the top of seawater surface. Then, the required amount of ZFO MNPs (0.01-0.05 g) was added to the top of the oil spill. After a period of 5 min, the ZFO MNPs containing the sorbed oil were collected using a permanent magnet. The oil removal experiments were triplicated and equation (8) was used to estimate the gravimetric oil removal (GOR , g/g), as follows;

$$GOR = \frac{m_2 - m_3}{m_1} \quad (8)$$

where m_1 is the mass of ZFO MNPs and m_2 is the total mass of the beaker (containing the oil spot, ZFO MNPs, and seawater) whereas m_3 stands for the mass of oil residue (beaker mass after removing ZFO MNPs-loaded tested oil).

3. Results and Discussion

3.1 Characterization of ZFO MNPs and oil samples

The XRD pattern of the ZFO MNPs prepared via the sol-gel process is shown in Figure-2. As can be seen from the XRD pattern, after burning the dried gel in air for 2 h at 600 °C, characteristic reflection planes with Miller indexes of (220), (311), (220), (400), (422), (511) and (440) were observed at 2θ values of 30.58°, 35.7°, 36.81°, 43.22°, 53.55°, 57.06° and 62.65°, respectively. These reflections confirm the formation of a cubic structure of the zinc ferrite (ZnFe_2O_4) phase (JCPDS card No. 79-1150) [37]. In addition, small amounts of impurities were observed in the XRD pattern, which were identified as $\alpha\text{-Fe}_2\text{O}_3$ and ZnO [37, 38]. The structural parameter values of ZFO MNPs, including lattice parameters (a), unit cell volume (V_{cell}), X-ray density (ρ_{XRD}), crystal size (D), and specific surface area (S_{XRD}), were estimated using XRD data of the high-intensity peak (311). The calculated values were about 8.3160 Å, 579.73 Å³, 5.52 g/cm³, 28.31 nm, and 38.39 m²/g for a , V_{cell} , ρ_{XRD} , D , and S_{XRD} , respectively.

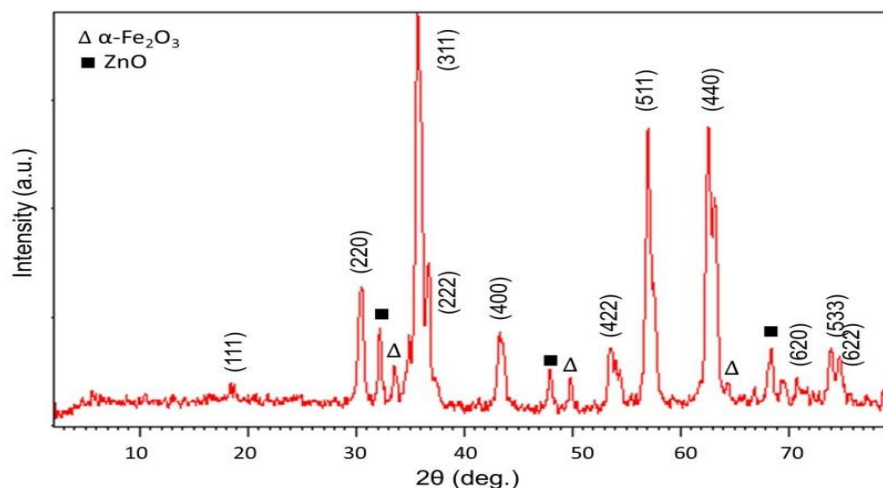


Figure 2- X-ray diffraction (XRD) pattern of ZnFe_2O_4 MNPs powder.

The magnetic force of the prepared material (ZFO MNPs) was found to be 40.22 mN. This value is similar to that reported for $\text{CoFe}_{1.9}\text{Zn}_{0.1}\text{O}_4$ MNPs (42.18 mN) [8] and higher than the one for maghemite/lignin-CNSL-formol nanocomposite (5.1 mN) [35]. The achieved magnetic force for ZFO MNPs was sufficient for removing the oil-loaded ZFO MNPs from the surface of water (Figure-6 c). In addition, the apparent density (ρ_a) of the ZFO MNPs was found to be 0.5287 g/cm^3 , which is lower than the density of seawater (1.0216 g/cm^3). This reported ρ_a value indicates that ZFO MNPs will float easily on the top of oil-contaminated surfaces [3, 36].

The FTIR spectra of the dried ash and ZFO MNPs (400 to 4000 cm^{-1}) are shown in Figure-3. It should be noted that both samples exhibit similar FTIR spectra. As shown (Figure-3b), the absorption bands located at 468 (ν_2) and 549 (ν_1) cm^{-1} could be ascribed to the bond vibrations of oxygen ion-octahedral metal ion (O-M_{Oct}) and oxygen ion-tetrahedral metal ion (O-M_{Tet}), respectively [39]. These characteristic bands are observed in FTIR spectra of most spinel ferrites and confirm their formation [40]. Within the wavenumber range (794 to 1385 cm^{-1}), the observed bands are assigned to NO_3^- vibration [41]. In addition, the band located at 1635 cm^{-1} is attributed to bending vibration of O-H bonds, while that observed at 3433 cm^{-1} is ascribed to stretching vibration of O-H bonds [16, 41].

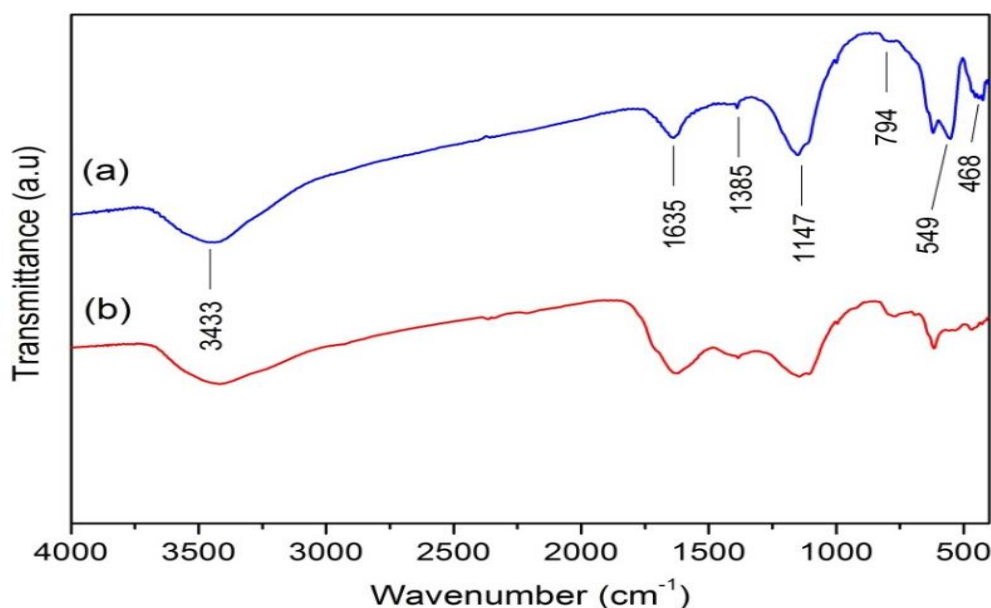


Figure 3 - FTIR spectra, (a) dried gel precursors (ash); (b) ZnFe_2O_4 MNPs.

Figure-4 displays the ATR-FTIR spectra of the selected oil samples (crude, gasoline, diesel and used motor oil) in the wavenumber ranging from 600 to 4000 cm^{-1} . It can be clearly seen that similar

ATR-FTIR spectra were observed for all tested oil samples. As shown, an absorption band that is accredited to CH_2 rocking vibration was observed at 722 cm^{-1} . The band located at 1046 cm^{-1} is attributed to the linkage of ester which is present in the asphaltene molecule. The absorption bands at 1372 and 1456 cm^{-1} are ascribed to C-H bonds bending vibration in methyl and methylene, respectively. The bands located at approximately 2854 and 2919 cm^{-1} , respectively, are assigned to stretching vibration of C-H bonds (asymmetric and symmetric) in aliphatic groups [42, 43].

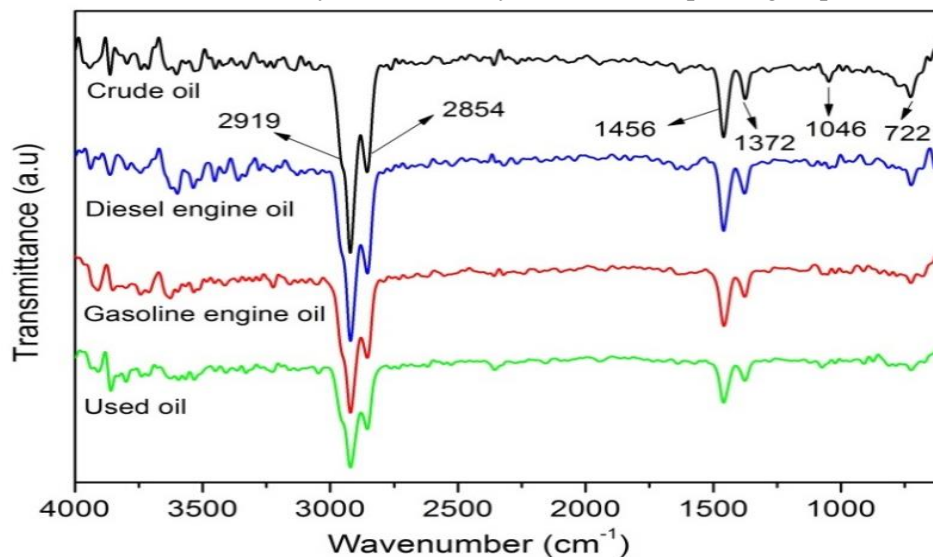


Figure 4 - ATR-FTIR spectra for the tested oil samples.

3.2 Gravimetric oil removal

Four different types of oily liquids, namely crude, gasoline engine oil, diesel engine oil, and used motor oil, were tested for gravimetric oil removal (*GOR*) experiments. Table-1 summarizes the main characteristics of the tested oils (*i.e.*, density and viscosity). As shown in the table, the densities of these oils are similar, but their viscosities are different. Figure-5 displays the *GOR* (g/g) values of the sorbate (tested oils) as a function of the amount of ZFO MNPs (sorbent). As shown, the *GOR* for all tested oil samples was decreased significantly with increasing the amount of ZFO MNPs from 0.01 to 0.05 g. When the sorbent mass was 0.01 g, the *GOR* values were about 23.00, 27.65, 22.62, and 30.54 g/g for crude, diesel engine, gasoline engine, and used motor oil, respectively. However, by increasing the sorbent amount to 0.05 g, the *GOR* values were decreased to 6.13, 7.42, 7.01, and 9.93 g/g for crude, diesel engine, gasoline engine, and used motor oil, respectively. The decrease in the *GOR* values by increasing the amount of the sorbent was also reported by others [8, 44]. For instance, the motor oil sorption capacity was reported to be decreased from 33 g/g to 23 g/g by increasing the sorbent (natural wool fibers) amount from 0.04 g to 0.18 g [44]. In another study, Amar *et al.* [8] reported the decrease in oil sorption capacity from 13.72 g/g to 5.5 g/g when the sorbent (spinel ferrite) amount was increased from 0.01 to 0.04 g. This decrease in the sorption capacity could be attributed to the aggregation of the sorbent materials. As a result, the surface area of the sorbent was decreased and oil spills were prevented from entering into the inner available pores for oil sorption [8]. Figure-6 presents images for the gasoline engine oil removal experiment using ZFO MNPs as a sorbent material. As shown, the magnetic sorbent loaded with gasoline oil was separated easily from the surface of seawater using a magnetic bar (Figure-6 c).

Table 1- The characteristics of the tested oils at 25 °C.

Tested oil	Viscosity (mPa s)	Density (g/cm ³)
Crude	39.30	0.8083
Diesel	29.50	0.8821
Gasoline	35.80	0.8913
used	16.00	0.8804

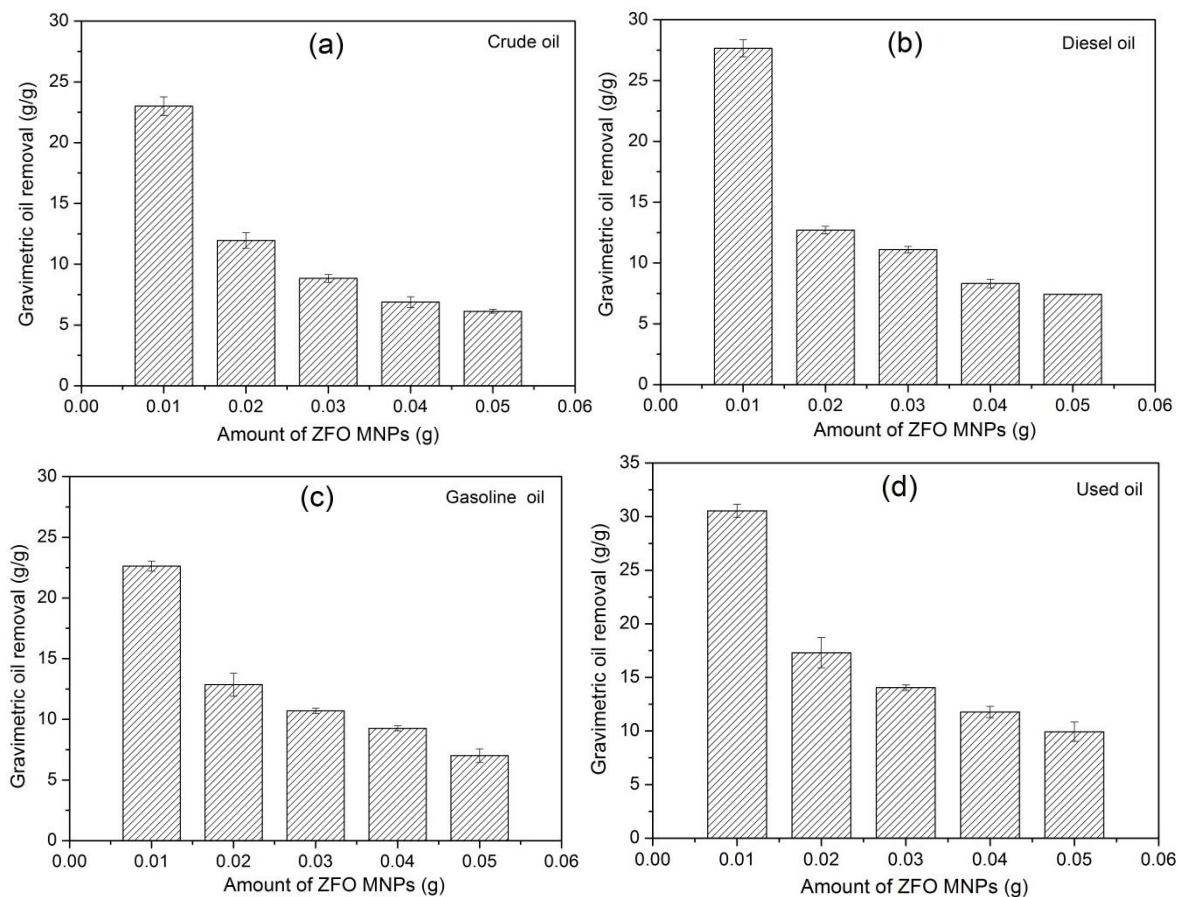


Figure 5- Relationship between the gravimetric oil removal and the amount of ZFO MNPs, (a) crude oil; (b) diesel oil; (c) gasoline oil; (d) used oil.

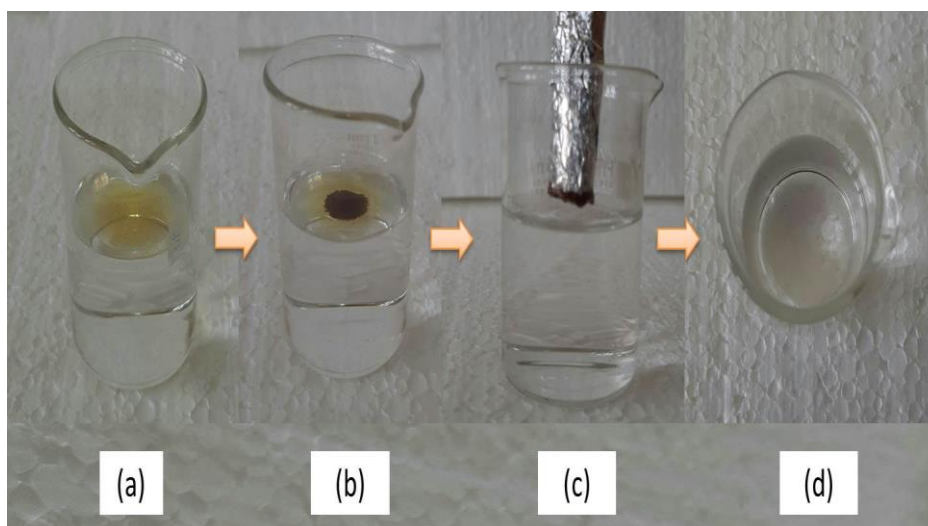


Figure 6 - Images showing gasoline oil removal test. (a) oil spill on seawater surface; (b) ZFO MNPs on the top of oil spill; (c) magnetic separation of ZFO MNPs loaded with oil spill; (d) seawater after oil removal test.

In general, the process of oil sorption is very complicated and depends on the properties of both the tested oil (*e.g.*, density, viscosity, *etc.*) and the sorbent material (*e.g.*, porosity, surface area, *etc.*). Figure-7 presents the relationship between the *GOR* or oil sorption capacity and the viscosity of the tested oil at two different sorbent amounts (0.01 and 0.05 g). As shown in the figure, oil samples with the lower viscosities exhibited the highest oil sorption capacities. When ZFO MNPs amount was 0.05

g (Figure-7 b), the oil sorption capacities were in the following order; used oil > diesel oil > gasoline oil > crude oil. The decreased oil sorption capacities for oils with higher viscosities could be due to the fact that high viscosity prevented oils from penetrating into the inner pores of the sorbent, resulting in low oil sorption capacity [45]. This implies that low viscosity is preferred for oil diffusion in the pores of the sorbent, providing high oil sorption capacities [46]. Thus, the used motor oil has a lower viscosity (16.00 mPa s) and, among the other tested oils, it exhibits the highest oil sorption capacities of 30.54 and 9.93 g/g when ZFO MNPs amounts were 0.01 g (Figure-7 a) and 0.05 g (Figure-7 b), respectively.

A literature-based comparison of the gravimetric oil removal of the prepared material (ZFO MNPs) with those of other magnetic nanosorbents [2, 28, 29, 47-49] is given in Table-2. As shown in the table, the gravimetric oil removal capacity of ZFO MNPs is comparable to those of other oil sorbents. These results demonstrate that the prepared material (ZFO MNPs) can be used as an oil sorbent for oil spillage cleanup from water surfaces. Although the proposed sorbent material (ZFO MNPs) exhibited an acceptable performance, the oil sorption capacity might be enhanced by improving the properties of the sorbent materials (e.g., surface area and porosity). This can be achieved using alternative methods to synthesize the sorbent material, such as the hydrothermal method. Beside the viscosity of the tested oil, water salinity and sorption time should be also investigated to address their influences on oil sorption capacity. In addition, the reusability of the proposed sorbent material should be taken into consideration as it plays an economic role in the whole oil removal process.

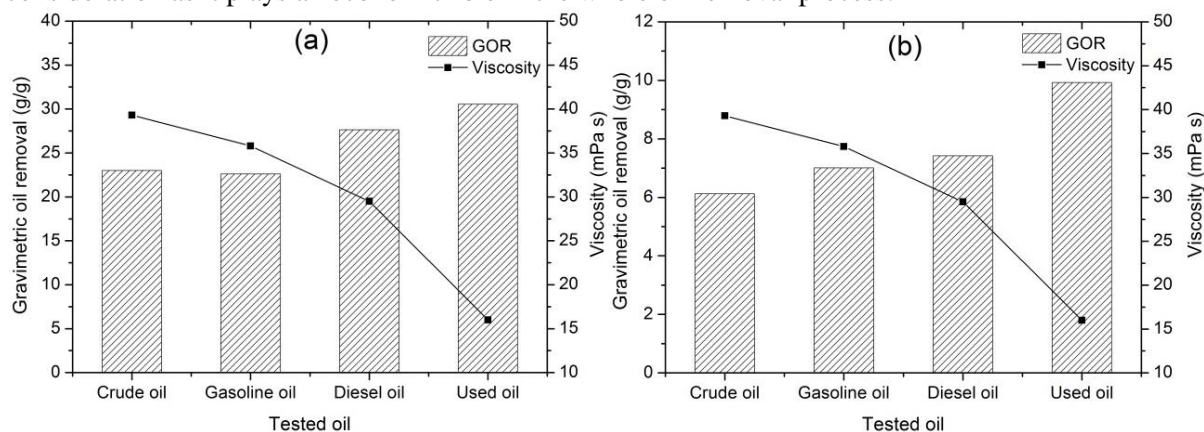


Figure 7- The gravimetric oil removal as a function of the viscosity for tested oils at different sorbent amounts. (a) 0.01 g of ZFO MNPs; (b) 0.05 g of ZFO MNPs.

Table 2- Comparison of the gravimetric oil removal for various magnetic sorbents, based on published literature.

Sorbent material	Type of oil	Gravimetric oil removal (g/g)	Reference
Fe_3O_4	Crude oil	2.16	[47]
$\gamma\text{-Fe}_2\text{O}_3/\text{resin}$	Crude oil	8.33	[48]
$\text{PS}/\text{NiFe}_2\text{O}_4$	Motor oil	15.11	[28]
$\text{PVDF}/\text{CoFe}_2\text{O}_4$	Motor oil	18.07	[2]
$\text{Fe}_3\text{O}_4/\text{Silica}$	Diesel oil	3.78	[49]
$\text{CoFe}_{1.9}\text{Zn}_{0.1}\text{O}_4$	Diesel oil	8.86-14.99	[8]
$\text{CoFe}_2\text{O}_4/\text{sawdust}$	Lubricant oil	11.50	[29]
$\text{CoFe}_{1.9}\text{Zn}_{0.1}\text{O}_4$	Hydraulic oil	5.24-10.58	[8]
ZnFe_2O_4	Crude oil	6.13-23.00	This study
ZnFe_2O_4	Diesel oil	7.42-27.65	This study
ZnFe_2O_4	Gasoline oil	7.01-22.62	This study
ZnFe_2O_4	Used motor oil	9.93-30.54	This study

PS = polysulfone, PVDF = Polyvinylidene .

4. Conclusions

In conclusion, ZFO MNPs were used as oil sorbent materials, after being synthesized via a sol-gel method and characterized using XRD and FTIR techniques. The XRD data revealed that ZFO MNPs and small amounts of impurities (α -Fe₂O₃ and ZnO) were obtained after burning their ash at 600 °C for 2 h. The oil sorption capability of ZFO MNPs was studied using crude oil, gasoline engine oil, diesel engine oil, and used motor oil as a water pollutant model. The prepared material exhibited a good magnetic property and a density value that is lower than that of seawater, allowing its easy magnetic separation and flotation. The oil sorption capacity of ZFO MNPs is related to the viscosity of the tested oil. The sorption capacity of the used motor oil, which has the lower viscosity, was higher than those of the other oily liquid samples. The results revealed that ZFO MNPs have a good combination of the magnetic property and the removal of oil spills from water surfaces.

Conflict of Interest

We have no conflict of interest to disclose.

References

1. Fingas, M. **2011**. *Oil Spill Science and Technology*. First Edition. Elsevier Inc.
2. Dorneanu, P.P., Cojocaru C., Olaru N., Samoila P., Airinei A. and Sacarescu, L. **2017**. Electrospun PVDF fibers and a novel PVDF/CoFe₂O₄ Fibrous Composite as Nanostructured Sorbent Materials for Oil Spill Cleanup. *Applied Surface Science*, **424**: 389-396.
3. Varela, A., Oliveira, G., Souza Jr F., Rodrigues, C. and Costa M. **2013**. New Petroleum Absorbers based on Cardanol-furfuraldehyde Magnetic Nanocomposites. *Polymer Engineering & Science*, **53**: 44-51.
4. Singh B., Kumar S., Kishore. B. and Narayanan, T.N. **2020**. Magnetic Scaffolds in Oil Spill applications. *Environmental Science Water Research & Technology*, In press. DOI: 10.1039/c9ew00697d
5. Atlas, R.M. **2011**. Oil Biodegradation and Bioremediation: A Tale of the Two Worst Spills in U.S. History. *Environmental Science & Technology*, **45**: 6709–6715.
6. Cao, E., Xiao, W., Duan, W., Wang, N., Wang, A. and Zheng, Y. **2018**. Metallic Nanoparticles Roughened Calotropis Gigantea Fiber Enables Efficient Absorption of Oils and Organic Solvents. *Industrial Crops & Products*, **115**: 272-279.
7. Broje, V. and Keller, A.A. **2007**. Effect of Operational Parameters on the Recovery Rate of an Oleophilic Drum Skimmer. *Journal of Hazardous Materials*, **148**: 136-143.
8. Amar, I A., Alshibani Z.M., Abdulqadir, M.A., Abdalsamed, I.A., Althamim, F.A. **2019**. Oil Spill Removal from Water by Absorption on Zinc-Doped Cobalt Ferrite Magnetic Nanoparticles. *Advanced Journal of Chemistry-Section A*, **2**: 365-376.
9. Kujawinski, E.B., Kido Soule, M.C., Valentine, D.L., Boysen, A.K., Longnecker, K., Redmond MC. **2011**. Fate of Dispersants Associated with the Deepwater Horizon Oil Spill. *Environmental Science & Technology*, **45**: 1298-1306.
10. Lin, Q., Mendelssohn I.A., Carney, K., Miles, S.M., Bryner, N.P., Walton, W.D. **2005**. In-Situ Burning of Oil in Coastal Marshes. 2. Oil Spill Cleanup Efficiency as a Function of Oil Type, Marsh Type, and Water Depth. *Environmental Science & Technology*, **39**: 1855-1860.
11. Bragg, J.R., Prince, R.C., Harner, E.J., Atlas, R.M. **1994**. Effectiveness of Bioremediation for the Exxon Valdez Oil Spill. *Nature*, **368**: 413-418.
12. Zhu, K., Shang, Y.Y., Sun, P.Z., Li, Z., Li, X.M., Wei, J.Q., Wang, K.L., Wu, D.H., Cao, A.Y., Zhu, H.W. **2013**. Oil Spill Cleanup from Sea Water by Carbon Nanotube Sponges. *Frontiers of Materials Science*, **7**: 170-176.
13. Jiang, J., Zhang, Q., Zhan, X., Chen. F. **2017**. Renewable, Biomass-Derived, Honeycomblike Aerogel as a Robust Oil Absorbent with Two-Way Reusability. *ACS Sustainable Chemistry & Engineering*, **5**: 10307-10316.
14. Kefeni, K.K., Mamba, B.B. and Msagati, T.A.M. **2017**. Application of Spinel Ferrite Nanoparticles in Water and Wastewater Treatment: A Review. *Separation and Purification Technology*, **188**: 399-422.

15. Gomez-Pastora, J., Bringas, E. and Ortiz, I. **2014**. Recent Progress and Future Challenges of High Performance Magnetic Nano-adsorbent in Environmental Applications. *Chemical Engineering Journal*, **256**: 187-204.
16. Stoia, M. and Muntean, C. **2015**. Preparation, Characterization and Adsorption Properties of MFe_2O_4 (M = Ni, Co, Cu) Nanopowders. *Environmental Engineering and Management Journal*, **14**: 1247-1259.
17. AL-Awadi, S.S., Shbeeb, R.T. and Chiad, B.T. **2018**. Effect of Silver Nanoparticles on Fluorescence Spectra of C480 dye. *Iraqi Journal of Science*, **59**: 502-509.
18. Khalaf, S.A. and Ali I.M. **2018**. Enhancement the Sensitivity of Zinc Sulfide Nanostructure Against NO_2 Toxic Gas by Loading Graphene. *Iraqi Journal of Science*, **59**: 2242-2248.
19. Farooq, S., Saeed, A., Sharif, M., Hussain, J., Mabood, F. and Iftekhar, M. **2017**. Process Optimization Studies of Crystal Violet Dye Adsorption onto Noval, Mixed Metal $Ni_{0.5}Co_{0.5}Fe_2O_4$ Ferrosipinel Nanoparticles using Factorial Design. *Journal of Water Process Engineering*, **16**: 132-141.
20. Amar, I.A., Sharif, A., Alkhayali, M., Jabji, M., Altohami, F. and Abdulqadir, M. **2018**. Adsorptive Removal of Methylene Blue Dye from Aqueous Solutions using $CoFe_{1.9}Mo_{0.1}O_4$ Magnetic Nanoparticles. *Iranian Journal of Energy and Environment*, **9**: 247-254.
21. Amar, I.A., Sharif, A., Ali, M., Alshareef, S., Altohami, F., Abdulqadir, M.A. and Ahwidi, M.M. **2020**. Removal of Methylene Blue from Aqueous Solutions using Nano-Magnetic Adsorbent Based on Zinc-Doped Cobalt Ferrite, *Chemical Methodologies*, **4**: 1-18.
22. Suzuki, Y. **2001**. Epitaxial Spinel Ferrite Thin Films. *Annual Review of Materials Research*, **31**: 265-289.
23. Angelakeris, M., Li, Z.A., Hilgendorff, M., Simeonidis, K., Sakellari, D., Filippousi, M., Tian, H. Van Tendeloo, G., Spasova, M., Acet, M. and Farle, M. **2015**. Enhanced Biomedical Heat-triggered Carriers via Nanomagnetism Tuning in Ferrite-based Nanoparticles. *Journal of Magnetism and Magnetic Materials*, **381**: 179-187.
24. Amar, I.A., Lan, R., Petit, C.T.G., Arrighi, V., Tao, S. **2011**. Electrochemical Synthesis of Ammonia Based on a Carbonate-oxide Composite Electrolyte. *Solid State Ionics*, **182**: 133-138.
25. Amar, I.A., Petit, C.T., Mann, G., Lan, R., Skabara, P.J., Tao S. **2014**. Electrochemical Synthesis of Ammonia from N_2 and H_2O Based on $(Li, Na, K)_2 CO_3-Ce_{0.8}Gd_{0.18}Ca_{0.02}O_{2-\delta}$ Composite Electrolyte and $CoFe_2O_4$ Cathode. *International Journal of Hydrogen Energy*, **39**: 4322-4330.
26. Hong, D., Yamada, Y., Sheehan, M., Shikano, S., Kuo, C.H., Tian, M., Tsung, C.K. and Fukuzumi, S. **2014**. Mesoporous Nickel Ferrites with Spinel Structure Prepared by an Aerosol Spray Pyrolysis Method for Photocatalytic Hydrogen Evolution. *ACS Sustainable Chemistry & Engineering*, **2**: 2588-2594.
27. Patil, J.Y., Nadargi, D.Y., Gurav, J.L., Mulla, I.S. and Suryavanshi, S.S. **2014**. Synthesis of Glycine Combusted $NiFe_2O_4$ Spinel Ferrite: A Highly Versatile Gas Sensor. *Materials Letters*, **124**: 144-147.
28. Cojocaru, C., Dorneanu, P.P., Airinei, A., Olaru, N., Samoila, P., Rotaru, A. **2017**. Design and Evaluation of Electrospun Polysulfone Fibers and Polysulfone/ $NiFe_2O_4$ Nanostructured Composite as Sorbents for Oil Spill Cleanup. *Journal of the Taiwan Institute of Chemical Engineers*, **70**: 267-281.
29. Gan, W., Gao, L., Zhang, W., Li, J., Cai, L. and Zhang, X. **2016**. Removal of Oils from Water Surface via Useful Recyclable $CoFe_2O_4$ /Sawdust Composites under Magnetic Field. *Materials & Design*, **98**: 194-200.
30. Ling, Y., Yu, J., Lin, B., Zhang, X., Zhao, L. and Liu, X. **2011**. A Cobalt-free $Sm_{0.5}Sr_{0.5}Fe_{0.8}Cu_{0.2}O_{3-\delta}-Ce_{0.8}Sm_{0.2}O_{2-\delta}$ Composite Cathode for Proton-conducting Solid Oxide Fuel Cells. *Journal of Power Sources*, **196**: 2631-2634.
31. Ismail, B., Hussain, S.T. and Akram, S. **2013**. Adsorption of Methylene Blue onto Spinel Magnesium Aluminate Nanoparticles: Adsorption Isotherms, Kinetic and Thermodynamic Studies. *Chemical Engineering Journal*, **219**: 395-402.
32. Ahmad, S.I., Ansari, S.A. and Kumar, D.R. **2018**. Structural, Morphological, Magnetic Properties and Cation Distribution of Ce and Sm Co-substituted Nano Crystalline Cobalt Ferrite. *Materials Chemistry and Physics*, **208**: 248-257.

33. Marques, F.D., Souza Jr, F.G. and Oliveira, G.E. **2016**. Oil Sorbers Based on Renewable Sources and Coffee Grounds, *Journal of Applied Polymer Science*, **133**: 43127.
34. Du, W., Dai, G., Wang, B., Li, Z. and Li, L. **2018**. Biodegradable Porous Organosilicone-modified Collagen Fiber Matrix: Synthesis and High Oil Absorbency, *Journal of Applied Polymer Science*, **135**: 46264.
35. Grance E.G.O., Souza Jr, F.G., Varela, A., Pereira, E.D., Oliveira, G.E. and Rodrigues, C.H.M. **2012**. New Petroleum Absorbers Based on Lignin-CNSL-formol Magnetic Nanocomposites. *Journal of Applied Polymer Science*, **126**: E305-E312.
36. Elias, E., Costa, R., Marques, F., Oliveira, G., Guo, Q., Thomas, S. and Souza Jr, F.G. **2015**. Oil-spill Cleanup: The Influence of Acetylated Curaua Fibers on the Oil-removal Capability of Magnetic Composites. *Journal of Applied Polymer Science*, **132**: 1-8.
37. Sun, S., Yang, X., Zhang, Y., Zhang, F., Ding, J., Bao, J. and Gao, C. **2012**. Enhanced Photocatalytic Activity of Sponge-like $ZnFe_2O_4$ Synthesized by Solution Combustion Method. *Progress in Natural Science: Materials International*, **22**: 639-643.
38. Kamari, H.M., Naseri, M.G. and Saion, E.B. **2014**. A Novel Research on Behavior of Zinc Ferrite Nanoparticles in Different Concentration of Poly(vinyl pyrrolidone) (PVP). *Metals*, **4**: 118-129.
39. Kumar, L., Kumar, P. and Kar, M. **2013**. Cation Distribution by Rietveld Technique and Magnetocrystalline Anisotropy of Zn Substituted Nanocrystalline Cobalt Ferrite. *Journal of Alloys and Compounds*, **551**: 72-81.
40. Amrutha, V.S., Anantharaju, K.S., Prasanna, D.S., Rangappa, D., Shetty, K., Nagabhushana, H., Ashwini, K., Vidya, Y.S. and Darshan, G.P. **2020**. Enhanced Sunlight Driven Photocatalytic Performance and Visualization of Latent Fingerprint by Green Mediated $ZnFe_2O_4$ -RGO Nanocomposite. *Arabian Journal of Chemistry*, **13**: 1449-1465.
41. Konicki, W., Sibera, D., Mijowska, E., Lendzion-Bieluń, Z. and Narkiewicz, U. **2013**. Equilibrium and Kinetic Studies on Acid Dye Acid Red 88 Adsorption by Magnetic $ZnFe_2O_4$ Spinel Ferrite Nanoparticles. *Journal of Colloid and Interface Science*, **398**: 152-160.
42. Wilt, B.K., Welch, W.T., Rankin, J.G. **1998**. Determination of Asphaltenes in Petroleum Crude Oils by Fourier Transform Infrared Spectroscopy, *Energy & Fuels*, **12**: 1008-1012.
43. Kumar, S. and Mahto, V. **2016**. Emulsification of Indian Heavy Crude Oil in Water for its Efficient Transportation Through Offshore Pipelines. *Chemical Engineering Research and Design*, **115**: 34-43.
44. Ognjanovic, V.R., Aleksic, G. and Rajakovic, L. **2008**. Governing Factors for Motor Oil Removal from Water with Different Sorption Materials. *Journal of Hazardous Materials*, **154**: 558-563.
45. Chu, Y., and Pan, Q. **2012**. Three-dimensionally Macroporous Fe/C Nanocomposites as Highly Selective Oil-absorption Materials. *ACS Applied Materials & Interfaces*, **4**: 2420-2425.
46. Tan, D., Zhao, J., Gao, C., Wang, H., Chen, G., Shi, D. **2017**. Carbon Nanoparticle Hybrid Aerogels: 3D Double-interconnected Network Porous Microstructure, Thermoelectric, and Solvent- Removal Functions. *ACS Applied Materials & Interfaces*, **9**: 21820-21828.
47. Debs, K.B., Cardona, D.S., da Silva, H.D.T., Nassar, N.N., Carrilho, E.N.V.M., Haddad, P.S. and Labuto, G. **2019**. Oil Spill Cleanup Employing Magnetite Nanoparticles and Yeast-based Magnetic Bionanocomposite. *Journal of Environmental Management*, **230**: 405-412.
48. Gomes de Souza Jr, F., Marins, J.A., Rodrigues, C.H. and Pinto, J.C. **2010**. A Magnetic Composite for Cleaning of Oil Spills on Water. *Macromolecular Materials and Engineering*, **295**: 942-948.
49. Yu, L., Hao, G., Liang, Q., Zhou, S., Zhang, N. and Jiang, W. **2015**. Facile Preparation and Characterization of Modified Magnetic Silica Nanocomposite Particles for Oil Absorption. *Applied Surface Science*, **357**: 2297-2305.